Cellulose (2023) 30:7235–7250
https://doi.org/10.1007/s10570-023-05331-4

ORIGINAL RESEARCH

Thiophene functionalized cellulose immobilized with metal organic framework for removal of heavy metals

Alaa M. Munshi · Nasser A. Alamrani · Hussain Alessa · Meshari Aljohani · Saham F. Ibarhiam · Fawaz A. Saad · Salhah D. Al-Qahtani · Nashwa M. El-Metwaly

Received: 7 August 2022 / Accepted: 15 June 2023 / Published online: 27 June 2023

Abstract Releasing of heavy metals within the wastewater of industries decreases the water quality and is dangerous for the human beings and other living organisms. In the current report, composite from metal organic framework (MIL-125-NH_2) and cellulosic filter paper (FP) was designed and applied in removal of heavy metals from water. The FP was firstly functionalized with thiophene-2-carboxylic acid giving TH@FP and subsequently grafted with MIL-125-NH_2 to obtain MIL@TH@FP composite. The all-synthesized materials were characterized and confirmed by using scanning microscopy, X-ray diffraction and infrared spectroscopy. These materials were employed in removal of heavy metals (Hg^{2+}, Cr^{3+}, Cu^{2+}) and the adsorption agreed with the order of FP < MIL@FP < TH@FP < MIL@TH@FP. The metal adsorption was fitted to the pseudo second order kinetics and Langmuir isotherm. After grafting with thiophene-2-carboxylic acid and MIL-125-NH_2, the metal adsorption onto FP was enhanced by a factor of 3.1–3.4. The maximum capacities of adsorption for Hg^{+2}, $Cr^{+3}$and Cu^{+2} onto MIL@TH@FP composite were 182.8, 109.7 and 134.1 mg/g, respectively. After reusing for five cycles, the metal adsorption capacity of MIL@TH@FP composite was only lowered by 12.8–22.8%, which reflected its stability and recyclability.

Keywords Cellulosic filter paper · MIL-125-NH_2 · Hg^{+2} · Heavy metals, water treatment · Recoverability

Supplementary Information The online version contains supplementary material available at https://doi.org/10.1007/s10570-023-05331-4.

A. M. Munshi · H. Alessa · F. A. Saad · N. M. El-Metwaly (✉)
Department of Chemistry, Faculty of Applied Sciences, Umm Al-Qura University, Makkah, Saudi Arabia
e-mail: n_elmetwaly00@yahoo.com; nmmohamed@uqu.edu.sa

N. A. Alamrani · M. Aljohani · S. F. Ibarhiam
Department of Chemistry, College of Science, University of Tabuk, Tabuk 71474, Saudi Arabia

S. D. Al-Qahtani
Department of Chemistry, College of Science, Princess Nourah Bint Abdulrahman University, P.O. Box 84428, Riyadh 11671, Saudi Arabia

N. M. El-Metwaly
Department of Chemistry, Faculty of Science, Mansoura University, Mansoura, Egypt

Introduction

A significant environmental hazard is heavy metals in water. Heavy metals as industrial wastes, agricultural wastes or from other human activities could be eliminated to the water body to cause risky environment and human health problems. Releasing of toxic chemicals from the wastewater of industries decreases the water quality to be dangerous to the human beings and other living organisms. Lead (Pb), chromium

(Cr), arsenic (As), cadmium (Cd), copper (Cu), nickel (Ni) and mercury (Hg), as heavy metals are commonly discharged within industrial wastewater. The toxic effect of heavy metals results in obstructive lung diseases, reducing the plant growth, causing cancer, organ damaging, nervous system damaging, and eventual death in some of extreme cases (Ahluwalia and Goyal 2007; Aksu 2005; Madadrang et al. 2012; Tesfaye 2016; WHO 2011). The heavy metals are categorized as risky pollutants owing to their severe toxic impacts. The existence of these hazardous heavy metals, even at low doses, affects the human and other living organisms' health (Bakhtiari and Azizian 2015; Cui et al. 2015). The progression of the industrial sector is the main cause of elimination of heavy metals in water, air, and soil, especially in the developing countries (Ahluwalia and Goyal 2007). Most of the industries such as, leather, tanneries, textile, metal, mining electroplating, batteries, chemical and petrochemical, ceramic, cement, paper, fertilizer and pesticides, act in eliminating their wastewater that contains different hazard heavy metals without any preliminary treatment into the surrounding environment. Hazard heavy metals such as cadmium, lead, and chromium could not be broken down in the surrounding environment, to be bioaccumulated in the kidneys and livers of invertebrates and vertebrates. Such risky heavy metals could cause carcinogenic effects for the bladder, kidney, brain, rectum, and colon. The maximum permitted values for cadmium, lead, and chromium in water is 0.003 mg/L, 0.01 mg/L, and 0.05 mg/L, respectively (WHO 2011). Mercury, as one of the heavy metals, is naturally occurring in the earth's crust, is also ascribed as one of the toxic environmental pollutants (Shahid et al. 2020). Mercury commonly existed in three different phases; inorganic mercury, organic mercury complexes and elemental (liquid) mercury. Inorganic mercury is existed in two oxidation states: mercury(I) and mercury(II). Three phases of mercury are reported to cause serious health problems to human beings (Park and Zheng 2012; Rice et al. 2014). Different inorganic mercury containing materials are known to be soluble in water, resulting in their persistence as one of the risky environmental pollutants in aquatic systems (Oehmen et al. 2014). Despite of the natural an abundance of mercury containing compounds in the environment, the phase and the concentration of mercury which released via the anthropogenic resources, like, the industrial activities, petrochemical production, and mining, are more toxic and causing a major environmental deterioration (Oehmen et al. 2014; Shahid et al. 2020). The combustion of hydrocarbons that releasing mercury into the atmosphere, whereas, wastewater from petrochemical facilities could discharge mercury into the hydrosphere.

Nowadays, the development of industrialization for any country is ascribed as a basic building block for the economy, but it has hazardous effect on the surrounding environment via the release of heavy metal ions (Sharma and Bhattacharya 2017) and other pollutants in the wastewater (Hoseinzadeh et al. 2021; Mahmoodi et al. 2014; Mahmoodi and Saffar-Dastgerdi 2019). Proper management of wastewater must be preceded by various wastewater management policies in order to inhibit harmful effects on the surrounding environment and on the human beings. Different treatment techniques like precipitation, ion exchange, membrane filtration, reversible osmosis, ultra-filtration, coagulation-flocculation, and flotation were widely applied for removing the heavy metals from the wastewater. However, these techniques are ascribed as highly cost and time-consuming procedures (Qasem et al. 2021). However, the adsorption or treatment strategies-based on the exploitation of an efficient sorbent were described as promising and effective techniques for water treatment for removing heavy metals (Rajasulochana and Preethy 2016). It was reported that zeolites and biomass-derivatized adsorbents like tea and coffee waste, saw dust, orange peel, peanut shells, papaya seed, rice husk, dry tree leaves and barks, coconut leaf and powder egg shell, and commercial activated carbon, were applied as adsorbents for removing the heavy metals from different wastewater systems (Hussain and Sheriff 2014; Jayaweera et al. 2018; Nguyen et al. 2013). However, most of the referred adsorbing reagents are limitedly applicable owing to their low stability, consuming longer reaction duration, higher calcinations temperature, not recyclable, and with relatively low surface area and porosity…etc… Moreover, the currently applicable systems for mercury removal in the market could be expressed to be very expensive and proceed via the utilization of non-reproducible metallic-based products. Subsequently, there is a requirement in the petrochemical industries for adsorbing reagents to remove mercury that could act better and with more cost effectiveness than the currently applicable

metallic-based adsorbing reagents (Liang et al. 2016; Liu et al. 2014; Mon et al. 2016, 2019; Yee et al. 2013). In recent years, metal–organic frameworks (MOFs), as porous/tailorable materials, with superior physical and chemical properties, inherent large surface areas, and tunable cavities, are exhibited with broad and comprehensive applicability than zeolite and the activated carbon (Dehghankar et al. 2021).

Removal of heavy metals from wastewater was performed in the current work using composite from MIL-125-NH_2as Ti containing metal organic framework (MOF) and cellulosic filter paper (FP). The FP was preliminary grafted with thiophene-2-carboxylic acid, and subsequently MIL-125-NH_2 was uploaded onto the modified FP to prepare MIL@TH@FP composite. The as-prepared composite was characterized by scanning electron microscope, energy dispersive X-ray, X-ray diffraction and FTIR. The formed materials were applied in removal of heavy metals (Hg^{2+}, Cr^{3+}, Cu^{2+}) from water. Kinetics and isotherm as key parameters were also studied. Recycling process of the applied materials was eventually studied.

Experimental part

Chemicals and materials

Thiophene-2-carboxylic acid (99%, Sigma-Aldrich), magnesium sulphate ($MgSO_4$, anhydrous ≥ 99.5%, Sigma-Aldrich), tetrahydrofuran (THF, ≥ 99.9%, Sigma-Aldrich), sulfuric acid (98%, El Naser pharmaceutical chemicals co.), titanium iso-propoxide (97%, Sigma-Aldrich), 2-aminoterephthalic acid (99%, Sigma-Aldrich), *N*,*N*-dimethyl formamide (99.9%, Sigma-Aldrich), ethanol (99.9%, Sigma-Aldrich),ammonium hydroxide (99.9%, Sigma-Aldrich),mercury (II) chloride ($HgCl_2$, Sigma-Aldrich), chromium(III) chloride ($CrCl_3{\cdot}6H_2O$, Sigma-Aldrich) and copper(II) nitrate ($Cu(NO_3)_2{\cdot}9H_2O$, Sigma-Aldrich) were all applied without further purification. Cellulosic filter paper (FP, thickness of 160 µm) was supported from the commercial suppliers.

Grafting of thiophene-2-carboxylic acid on FP

THF (250.0 mL) was added to chemical reactor. To this reactor, 250 µL of sulfuric acid (as catalyst), 50.0 g (0.4 mol) of thiophene-2-carboxylic acid, 10.0 g of FP and 5.0 g (0.04 mol) of $MgSO_4$ were added. The homogenized mixture was allowed to react at 60 °C for 72 h. The solid product obtained was separated then cleaned with distilled water and ethanol to separate the unreacted thiophene-2-carboxylic acid and sulfuric acid. Washing process was continued until a neutral wash-out was obtained. Pure TH@FP was dried at 65 °C in a vacuum oven and stored in tight container until being used.

Grafting of MIL-125-NH_2 on FP and TH@FP

MIL-125-NH_2 was freshly prepared by using the method reported in literature (Abdelhameed et al. 2020). Afterwards, the prepared MIL-125-NH_2 was included within FP and thiophene modified FP (TH@FP) by self-assembly technique. 10 g of FP (or TH@FP) was individually reacted with 1 g of MIL-125-NH_2 powder in 100 mL DMF. The reactants were heated up to 50 °C for 30 min. The products (MIL@FP&MIL@TH@FP) were removed, washed with ethanol and then dried at room temperature prior to analysis and application.

The grafting percentage and grafting efficiency were determined as (Tyagi et al. 2009):

$$\%Grafting\,(\%G) = \frac{W_a - W_b}{W_b} \times 100$$

$$\%Grafting\ efficiency\,(\%GE) = \frac{W_a - W_b}{(W_a - W_b) + W_m} \times 100$$

where W_b and W_a are weight of the FP before and after the grafting process, respectively, and W_m is the weight of MILs.

Instrumental characterization

The topographical features of the untreated FP and the modified FP were investigated via Scanning Electron Microscope (SEM, Hitachi SU-70) running at 25 kV as accelerating voltage in room temperature. The elemental analyses of the prepared samples were also performed via the field emission gun energy dispersive X-ray spectrometer (EDX) analyzer equipped with the same microscopy. CSNH contents in FP and modified FP were determined on a LECO CHNS-932 element analyser. X-ray diffraction analysis

was performed for untreated FP and modified FP at room temperature. Samples were subjected to XRD, Philips X'Pert MPD diffractometer (Cu Kα X-radiation at 40 kV, 50 mA and λ = 1.5406 Å). Data of diffraction were estimated in range of 2θ = 3.5 to 50°. Infrared spectral results of untreated FP and modified FP before and after adsorption of heavy metals, were estimated via attenuated total Reflection-Fourier transform infrared spectroscopy (ATR-FTIR, Mattson 5000 FTIR spectrometer). FTIR instrument was operated with a detector of deuterated triglycine sulfate and accessory attenuated total reflectance (ATR unit with Golden Gate diamond crystal). The absorption spectra were estimated at wavenumber ranged in 500–4000 cm^{-1}.

Heavy metal ions adsorption

Certain amount of metal salts ($HgCl_2$, $CrCl_3$, $Cu(NO_3)_2$) were dissolved in the deionized water to prepare Hg^{2+}, Cr^{3+}, Cu^{2+} ions solution (100 ppm). To 10.0 mL of this solution, 0.01 g of FP and modified FP (TH@FP, MIL@FP and MIL@TH@FP) were separately added at normal temperature (30 °C) and neutral pH (6.8). After intervals of 30 min, solution was withdrawn from the test sample to determine the concentration of the non-adsorbed Hg^{2+}, Cr^{3+}, and Cu^{2+} ions. All experiments were performed in sets of three each to establish the reproducibility of the results. Influence of initial metal ion concentration (1–200 ppm) on the capacity of adsorption was studied at 30 min. To study the maximum removal capacity of heavy metal onto FP and modified FP, the same sample was repeatedly used 150 ppm of metal ion solution at the optimized conditions of time, temperature and pH. The reusability studies were also carried out by stripping-off the adsorbed metal ions with HCl to regenerate the used MOF@TH@FP each time before reusing. MOF@TH@FP was regenerated by immersed in 0.1 N HCl using 1:25 of material to liquor ratio for one hour under continuous stirring.

Statistical analyses

Adsorption data estimated in the current approach was an average of three independent measurements. Kinetics of adsorption, correlation coefficient (R^2) and standard deviations were all estimated via 2016 Microsoft Excel. All of the represented figures were drawn by applying origin 8 program and the error bars were presented within all figures.

Results and discussion

MIL@TH@FP

Before adding of MIL-125-NH_2 MOF, the cellulosic FP was firstly grafted with thiophene-2-carboxylic acid to prepare TH@FP. As suggested in Fig. 1, esterification reaction was carried out between cellulosic FP and thiophene-2-carboxylic acid. In the presence of sulfuric acid as dehydrating agent and $MgSO_4$ as catalyst, thiophene-2-carboxylic was bonded with cellulose forming TH@FP as ester and water molecule was produced. Afterwards, the synthesized TH@FP was interacted with MIL-125-NH_2 through ester groups. TH@FP can act as another ligand capable of forming coordination bonding with Ti of in MIL-125-NH_2. Hence, during self-assembly of MIL-125-NH_2within FP matrix, Ti might form a bond with 2-aminoterphethalic acid from one side and with TH@FP from the other side (Abdelhameed et al. 2017, 2018; Emam and Abdelhameed 2017a, b). The estimated elemental content from the elemental analysis was summarized in Table S1. The sulfur content in TH@FP was 4.79% confirmed that the grafting efficiency of TH onto FP was 32% achieving substitution degree of ≈1. While the estimated grafting efficiency of MIL-125-NH_2 onto FP and TH@FP was 12% and 22%, respectively. The practical image for FP, TH@FP, and MIL@TH@FP were shown in Fig. S1.

SEM

The topographical features of the FP surface before and after grafting with thiophene-2-carboxylic acid, also before and after uploading with MIL-125-NH_2, were examined by electron microscopy (SEM) and EDX (Fig. 2a–d). The plotted electronic images and EDX analysis affirmed that grafting of cellulose FP with thiophene-2-carboxylic acid. Particles of thiophene-2-carboxylic acid were seen over the clean surface of FP. The signal of sulfur was recorded at 2.2 eV. Incorporation of MIL-125-NH_2 within FP/grafted FP was affirmed (Fig. S2). Crystalline/cracks like structure MIL-125-NH_2 was observed to be

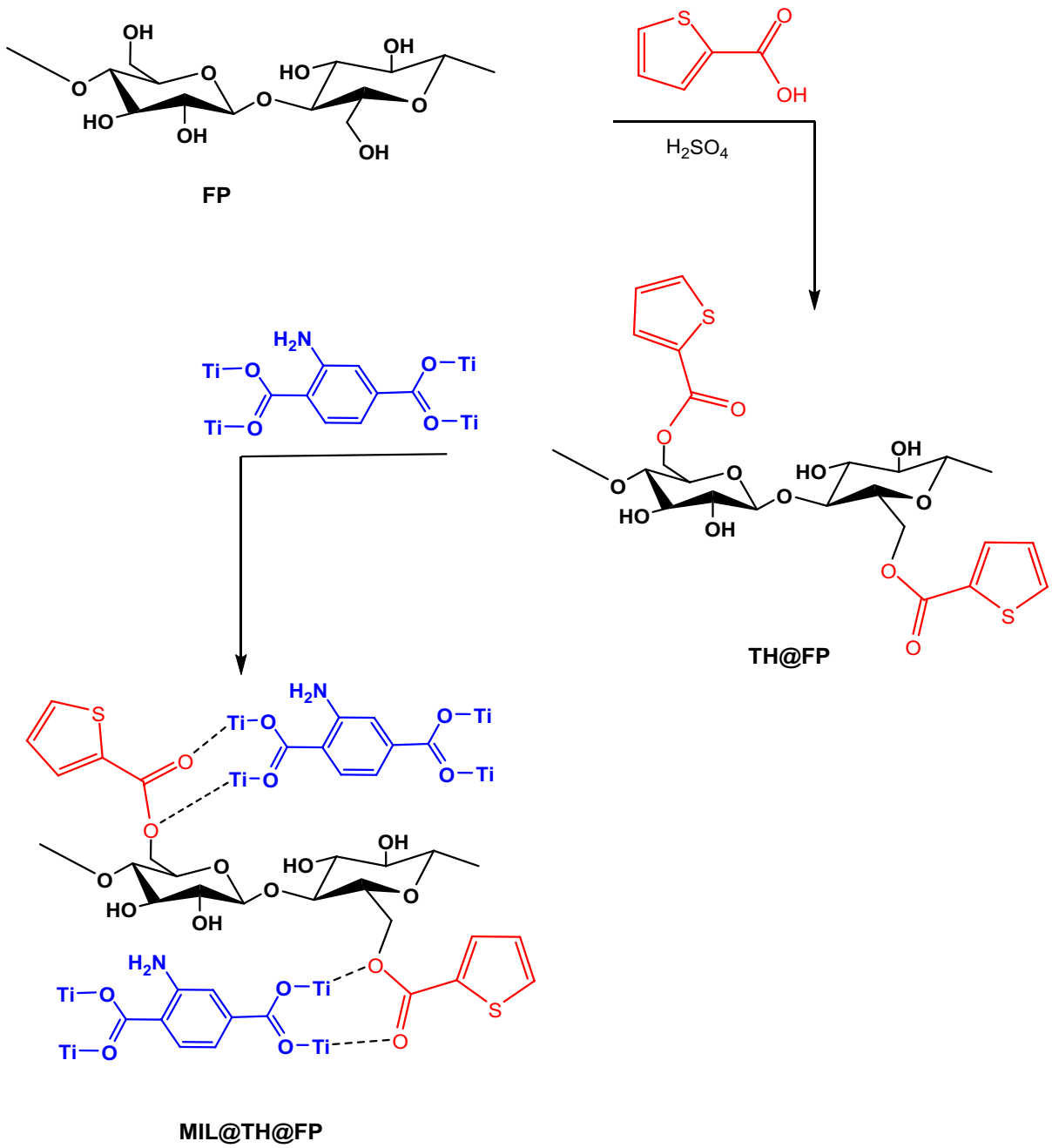

Fig. 1 Preparation scheme of MIL@TH@FP composite

successively uploaded on the surface of the grafted FP in case of MIL@TH@FP (Fig. 2d), while smaller sized with lower masses were shown on the surface of FP in case of MIL@FP (Fig. 2c). Signal of Ti element at 4.3 eV was detected in EDX spectra for both of MIL@FP and MIL@TH@FP. The microscopic observations approved the effect of grafting with thiophene for enhancing the affinity of cellulosic FP in MOF incorporation with higher amounts, which is related to the contribution of the accessible functional groups for thiophene in successive immobilization of MOF. The data of MOF/Ti contents were further

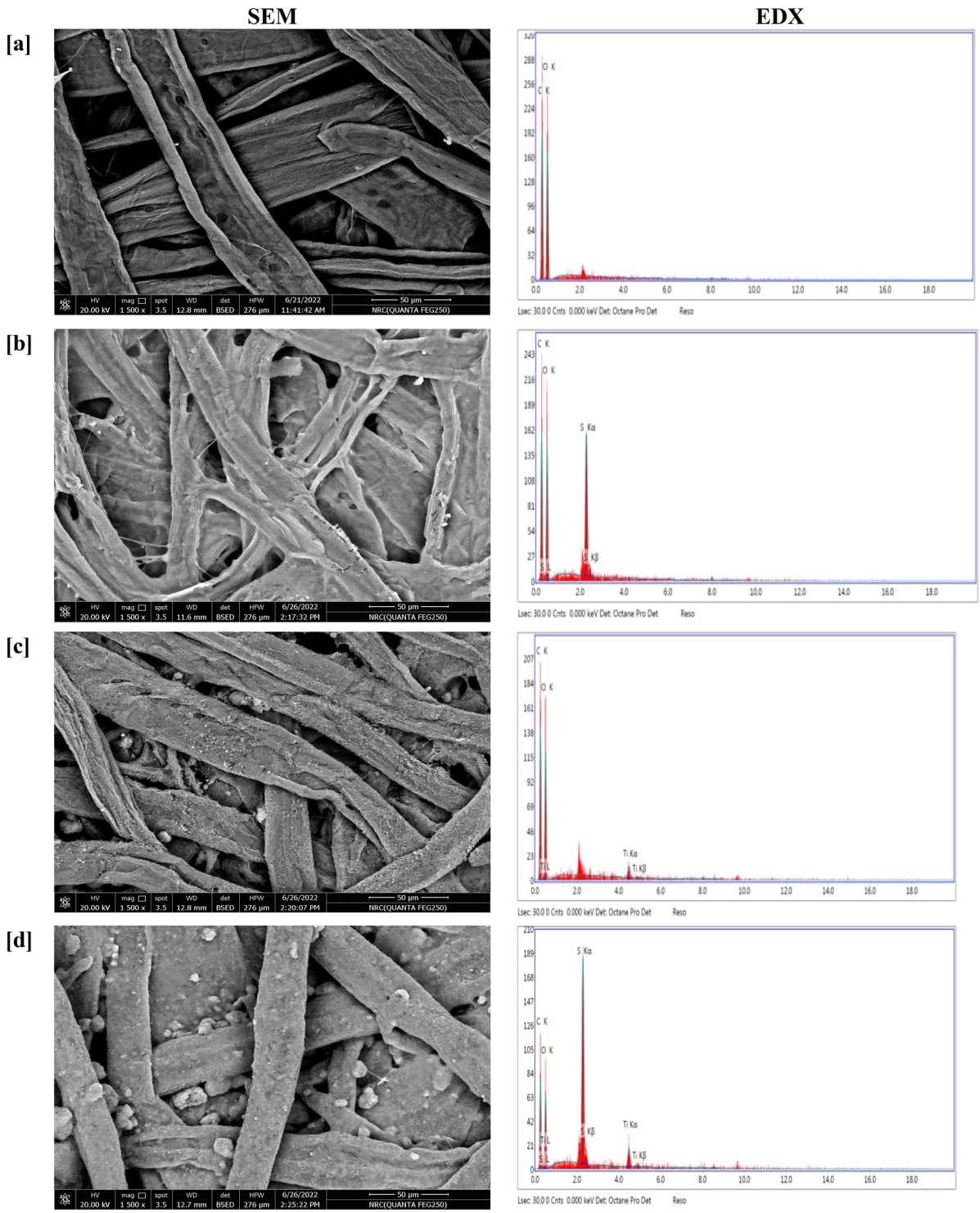

Fig. 2 Scanning electron microscopic images and EDX analysis for the synthesized materials; **a** FP, **b** TH@FP, **c** MIL@FP and **d** MIL@TH@FP

affirmed this hypothesis, where, TH@FP showed much higher materials content compared to FP.

XRD

Further confirmation for the successive assembly of MIL-125-NH_2 within FP/grafted FP matrix was obtained via X-ray diffraction analysis (Fig. S3). For MOF powder, several diffraction peaks were estimated at 2θ = 6.8°, 9.7°, 11.6°, 15.3°, 16.7°,17.9°, 19.4° and 22.5°, which were characterized for the crystalline MIL-125-NH_2 (Abdelhameed et al. 2020; Emam and Abdelhameed 2017a). FP exhibited the characteristic signals corresponding to the crystalline structure of cellulose I (Emam et al. 2017a, b, c) at 2θ = 15.2°, 16.7° and 23.1°. After grafting with thiophene, the diffraction of FP was not changed, meaning that, the crystalline structure of cellulose was not affected. In case of MIL@FP and MIL@TH@FP composite, most of diffraction peaks for MIL-125-NH_2 were clearly observed, besides the diffraction peaks of FP, which affirmed the successive immobilization of MIL-125-NH_2 MOF within the FP and modified FP.

FTIR

The chemical composition of the FP before/after grafting with thiophene-2-carboxylic acid and before/after immobilization of MIL-125-NH_2 was investigated by FTIR spectroscopic analysis as represented in Fig. S4. The characteristic absorption bands of FP for stretching vibration of OH, asymmetric stretching vibration of CH aliphatic, stretching vibration of C=O, and scissoring vibration of CH_2, were obviously detected at 3321–3261, 2874, 1606 and 1304–1375 cm^{-1}, respectively (Abdelhameed et al. 2016; Ahmed and Emam 2016; Emam and Bechtold 2015; Emam et al. 2015, 2016). For TH@FP, in addition to the as-mentioned characteristic bands of FP, the specialized absorption bands of thiophene were also represented, whereas, an absorption peak at 1567 cm^{-1} that is characteristic of carbon–carbon double bond (C=C) presented in the aromatic ring of thiophene, in addition to the absorption peak at 1445 cm^{-1}, corresponding to ring vibrations resulted from the symmetric stretching of the carbon–carbon double bonds in the thiophene moieties. Also, indicative peaks for carbon–sulfur double bond (C=S) stretching at 1012–1103 cm^{-1}, sulfur-containing functional groups including carbon–sulfur bond stretching were estimated at 737 cm^{-1} and C=O (carboxylate) at 1602 cm^{-1} (Annenkova et al. 1984; Fila et al. 2018; Luo et al. 2012). After grafting with MOF, the characteristic absorption peaks of MIL-125-NH_2 were clearly appeared beside the peaks of FP/TH@FP. For MIL@FP, the absorption peaks of amide I, II and III were detected at 1639, 1531 and 1246 cm^{-1}, respectively (Emam and Abdelhameed 2017a; Emam et al. 2020). Additionally, the vibration of Ti–O bond was recorded at 764 cm^{-1} and the absorption band of NH stretching vibration was overlapped with that of OH. In case of MIL@TH@FP, the absorption bands of MIL-125-NH_2 and thiophene were appeared beside the absorption peaks of FP, approving the successive assembly of MOF and thiophene within the FP. As a conclusion, the MIL-125-NH_2 is assumed to be coordinatively bonded with TH@FP via its function groups; hydroxyl and carbonyl groups.

Removal of heavy metals

Chromium (Cr), copper (Cu) and mercury (Hg) as heavy metals are commonly existed within the wastewater discharged from different industries. The toxic impact of heavy metals results in reduction of the growth and reproduction of plant, obstructive lung disease, carcinogenic effects, organ damaging, nervous system damaging, and eventually with high doses it could lead to death (Ahluwalia and Goyal 2007; Aksu 2005; Madadrang et al. 2012). Moreover, chromium ion does not break down in the environment, to be bio-accumulated within the kidneys and livers of invertebrates and vertebrates, whereas, the existence of mercury in water could cause serious health problems to human beings affecting the lungs, nervous system, and kidneys (Park and Zheng 2012; Rice et al. 2014). In recent years, there were researching reports of immobilizing sulfur based-accessible groups MOFs, as an approach for enhancing their adsorption action via Hg–S interaction (Liang et al. 2016; Liu et al. 2014; Mon et al. 2016, 2019; Yee et al. 2013). Post-synthetic modification reaction via thiol–ene, ‘‘click” reactions is ascribed as a method for anchoring thiol-functional groups within the cavities of the porous material (Ke et al. 2011; Li et al. 2019; Luo et al. 2015; Wang et al. 2019) that were effective materials exhibited with high mercury

removal capacity (Yin et al. 2018). However, such materials produced via thiol, ene reactions are limitedly applied attributed to the harsh synthetic conditions and the expensiveness of the reagents. In the presented approach, the accessibility of MIL@TH@FP composite as solid supporting template for wastewater treatment is currently approved via removal of heavy metals of Hg^{2+}, Cr^{3+}, Cu^{2+} ions that were selected as toxic pollutants in wastewater. FP and TH@FP as references were used for comparing their affinity by the prepared composite for heavy metals removal. Figure 3 showed the microscopic images for the prepared composite of MIL@TH@FP after its exploitation in removal of metal ions (Hg^{2+}, Cr^{3+}, Cu^{2+}) from wastewater. It could be obviously observed that, successive adsorption of the mentioned metal ions was shown on the surface of the exploited composite. Additionally, EDX data also showed the characteristic individual signals for Hg^{2+}, Cr^{3+} and Cu^{2+} at 2.2/9.9, 0.4/5.2 and 0.9/8.0 eV, respectively. Moreover, the adsorption of Hg^{2+}, Cr^{3+}, Cu^{2+} ions from wastewater onto the prepared composite was further approved via the infrared spectral results as represented in Fig. 4. After adsorption of metal ions

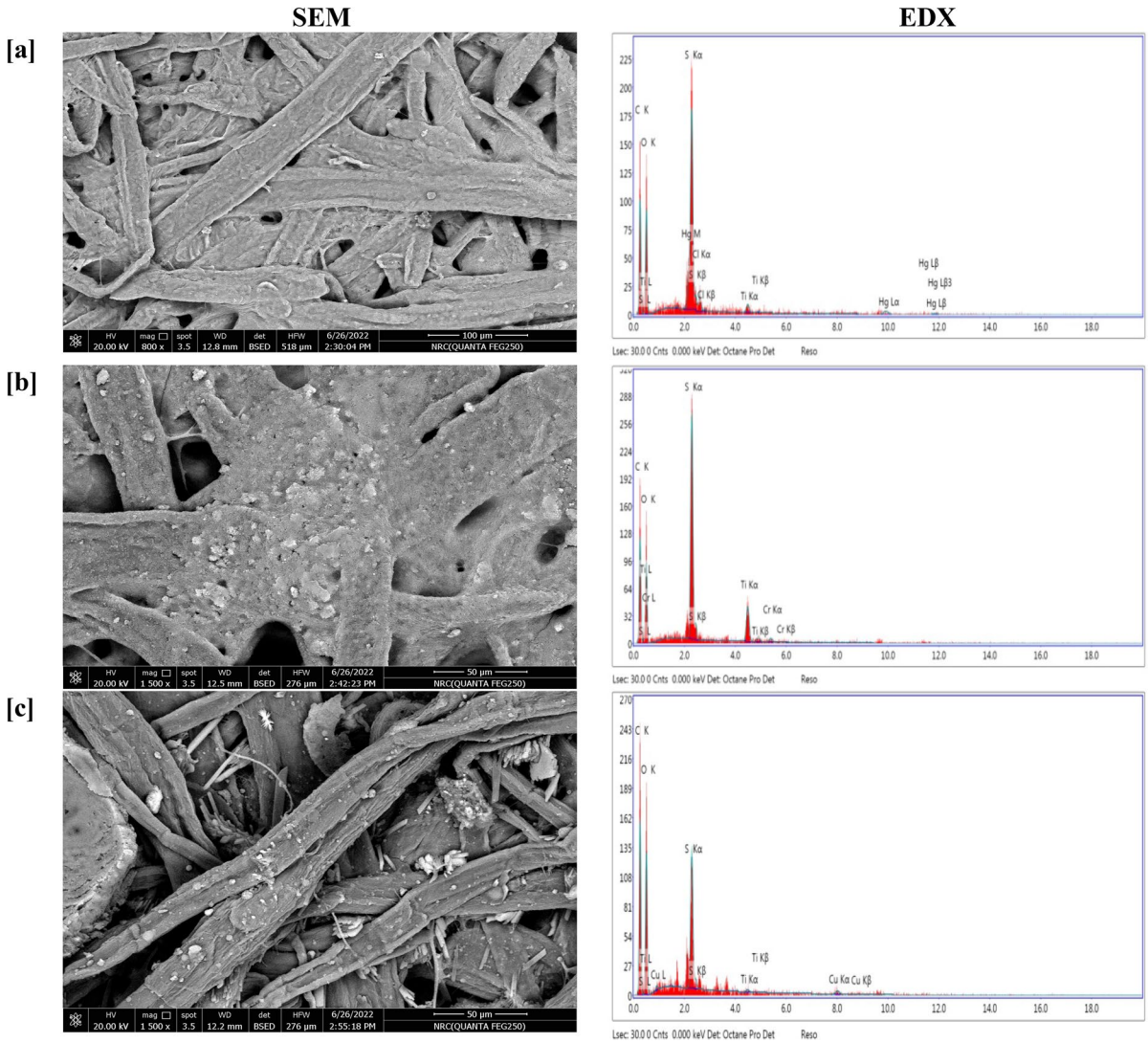

Fig. 3 Scanning electron microscopic images and EDX analysis for the synthesized composite after adsorption of metals; **a** Hg^{+2}@MIL@TH@FP, **b** Cr^{+3}@MIL@TH@FP and **c** Cu^{+2}@MIL@TH@FP

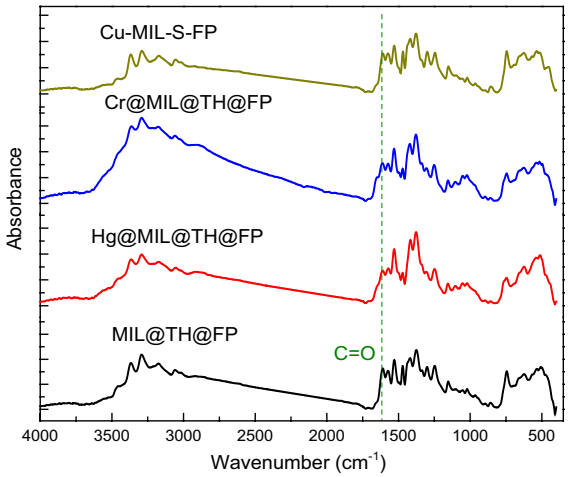

Fig. 4 FTIR spectra for the synthesized materials after adsorption of metals

onto MIL@TH@FP composite, the absorption peaks of M–O (Hg–O, Cr–O, Cu–O) were overlapped with that of C–S and Ti–O bonds at 730–770 cm^{-1}.

Adsorption kinetics

Adsorption kinetics of heavy metals (Hg^{2+}, Cr^{3+}, Cu^{2+}) onto the currently prepared adsorbents; i.e., FP, TH@FP, MIL@FP and MIL@TH@FP were studied and the data were plotted in Fig. 5. From the plotted data, it could be declared that, whatever the applied adsorbent type and adsorbed metal ion, the adsorption capacity was gradually increased with prolongation of reaction duration and the adsorption rates were fast in the first 30 min, attributing to the availability of the possible active sites. Regardless to the type of the currently exploited adsorbing reagent, the adsorption capacity for Hg was the highest because of the higher affinity of thiophene as sulfur containing moieties on the grafted FP towards Hg^{+2} rather than the other metals. The currently adsorption capacities were followed the order of MIL@TH@FP > TH@FP > MIL@FP > FP. From the estimated data in Fig. 5, it could be depicted that, the adsorption capacities of Hg^{+2} were gradually increased from 41 to 51 mg/g for FP to 129 and 174 mg/g for MIL@TH@FP after 30 and 120 min, respectively. While, the adsorption capacities for Cr^{+3} and Cu^{+2} were increased from 20 to 30 to 76 and 101 mg/g and from 21 to 35 to 83 and 110 mg/g, respectively after 30 and 120 min. After grafting with thiophene and MIL-125-NH_2, the adsorption capacities of metal ions onto FP were enhanced by factor of 3.1–3.4.

The non-liner fitting of pseudo-second ordered kinetics for the metal adsorption onto the applied materials was introduced in Fig. 5. The kinetic parameters (the constant rate of adsorption K_2, adsorption at equilibrium Q_e and relation coefficient R^2) were all estimated and tabulated in Table 1. The adsorption of metal ions (Hg^{2+}, Cr^{3+}, Cu^{2+} ions) onto the applied materials (FP, TH@FP, MIL@FP, MIL@TH@FP) were evaluated to be fitted well with pseudo-second order model, owing to linearity ($R^2 = 0.95–0.99$) and close experimental Q_e values to the theoretical Q_e values. The rate constant (K_2) of Hg^{2+} adsorption was observably decreased from 2.23×10^{-3} L/mg min for FP to 0.40×10^{-3} L/mg min for MIL@TH@FP. However, the rate constant (K_2) for Cr^{3+} & Cu^{2+} adsorption was diminished from 0.96×10^{-3} to 1.24×10^{-3} L/mg min for FP to 0.59 and 0.83×10^{-3} L/mg min for MIL@TH@FP, respectively. These results clarified that the adsorption rate of heavy metals onto TH@FP was significantly speeded up by grafting with MIL-125-NH_2, whereas, MIL@TH@FP showed the fastest adsorption rate. For all the examined samples, the mercury ion adsorption rate was mainly higher than that for copper and chromium ions. Based on the principle of pseudo-second order reaction, the adsorption of such metal ions onto the applied adsorbents was performed via a pseudo-chemical interaction (Fig. S5). Subsequently, the adsorption amounts were depended on the number of the accessible sites, that were increased by MIL-125-NH_2 impregnation and hence, further enhancement in the adsorption capacity could be realized via the increment of the grafted amount of MIL-125-NH_2 MOF within fabrics.

Adsorption isotherm

Adsorption isotherm of metals onto the synthesized materials was studied through plotting the adsorbed amounts (Q_e, mg/g) with the initial concentration of the studied metals (Fig. 6). Regardless to the adsorbed metals and adsorbent type; a plateau shaped figure was notified in all results. Adsorption amounts of metal ions were gradually increased until the saturation stage, to give plateau profile. The highest adsorption capability was observed for mercury

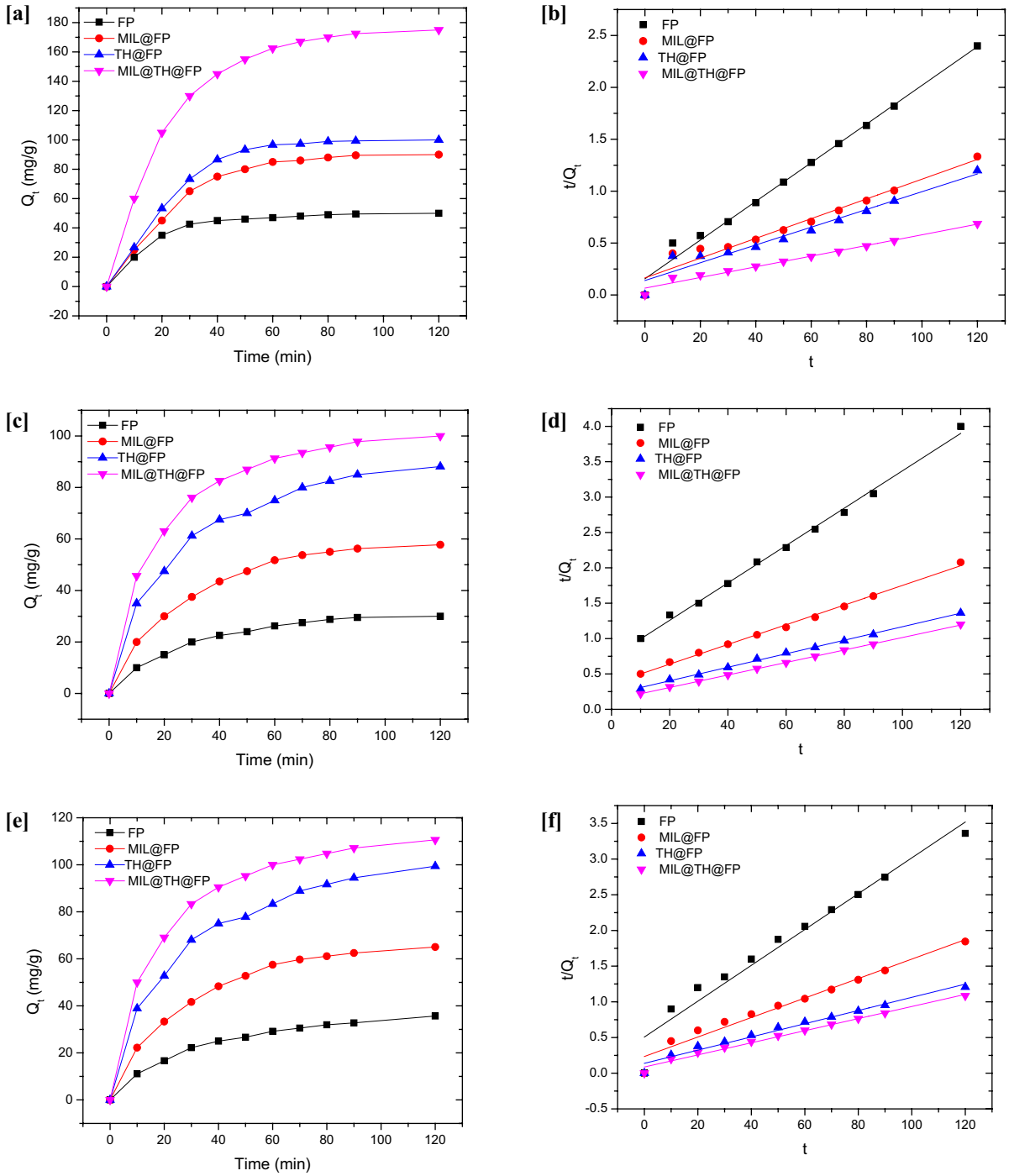

Fig. 5 Kinetic for adsorption of metals onto the synthesized materials; **a**, **b** Hg^{+2}, **c**, **d** Cr^{+3}, **e**, **f** Cu^{+2}, **a**, **c**, **e** effect of time and **b**, **d**, **f** linear fitting for pseudo-second order

Table 1 Kinetic parameters for metal adsoprtion onto the synthesized materials

Metal ions	Samples	$Q_e$exp. (mg/g)	Pseudo-first-order			Pseudo-second-order		
			Q_e (mg/g)	K_1 ($\times 10^3$, min^{-1})	R^2	Q_e(mg/g)	K_2 ($\times 10^3$, L/mg min)	R^2
Hg^{+2}	FP	51.0	2.55	1.97	0.58	53.65	2.23	0.99
	MIL@FP		2.53	4.93	0.74	105.15	0.55	0.95
	TH@FP		2.51	5.73	0.71	116.82	0.53	0.95
	MIL@TH@FP	174.0	2.44	17.80	0.87	194.55	0.40	0.98
Cr^{+3}	FP	30.0	2.58	1.26	0.78	37.85	0.96	0.99
	MIL@FP		2.56	2.67	0.78	71.89	0.53	0.99
	TH@FP		2.53	3.50	0.80	104.60	0.43	0.99
	MIL@TH@FP	101.0	2.50	5.02	0.72	113.25	0.59	0.99
Cu^{+2}	FP	35.0	2.58	1.49	0.82	39.84	1.24	0.95
	MIL@FP		2.55	3.06	0.80	73.26	0.80	0.97
	TH@FP		2.52	5.18	0.83	108.11	0.62	0.97
	MIL@TH@FP	110.0	2.49	5.85	0.75	117.92	0.83	0.99

ions while the lowest adsorption capacity was seen for chromium ions. The linear relationship for isotherm fitting was presented in Fig. 6 (Langmuir) and supplementary file (Fig. S6, Freundlich) and the isotherm parameters were all calculated and tabulated in Table 2. The best linearity ($R^2 = 0.99$) was achieved in case of Langmuir isotherm, to confirm that, the adsorption of such metal ions onto MIL@TH@FP was well fitted to Langmuir model. For all metal adsorption, the Langmuir rate constant (K_L) was significantly increased after grafting of FP with thiophene and MIL-125-NH_2. The values of K_L were raised from 178.97×10^{-3} to 821.32×10^{-3} mg/L for Hg^{+2}, from 146.99×10^{-3} to 259.17×10^{-3} mg/L for Cr^{+3} and from 106.02×10^{-3} to 154.01×10^{-3} mg/L for Cu^{+2}, in case of FP and MIL@TH@FP, respectively. The calculated maximum capacities (Q_{max}) for Hg^{+2}, $Cr^{+3}$and Cu^{+2} were observably increased from 57.3, 35.8 and 43.9 mg/g for FP to 182.8, 109.7 and 134.1 mg/g for MIL@TH@FP, respectively. After grafting with thiophene and MIL-125-NH_2, the maximum capacity of FP was improved with 3.2, 3.1 and 3.1 times for Hg^{+2}, Cr^{+3} and Cu^{+2} respectively. The presented Langmuir isotherm for adsorption of metals is characterized by the formation of one adsorption layer onto the homogenous surface of the absorbent (Abdelhameed et al. 2016; Bolster and Hornberger 2007; Emam et al. 2018). Whereas, during the adsorption reaction, the metal ions are assumed to be removed via the binding sites of MIL@TH@FP composite and within the intermolecular cavities. Therefore, the adsorption is limitedly affected by the affinity of the binding sites, whereas, every metal ion moiety is typically adsorbed on only one active site within the adsorbed layer (Abdelhameed et al. 2016, 2017, 2018; Emam et al. 2018). It could be summarized that, adsorption capacities of MIL@TH@FP against the studied metal ions were the highest compared to FP, MIL@FP and TH@FP, while, its affinity towards Hg^{+2} was observed to be higher than Cr^{+3} and Cu^{+2}.

Recoverability of MIL@TH@FP composite

The recoverability of adsorbents to be reused for repeated cycles with sufficient adsorption capacity is an important sector to be wide scaled applied. Different reports were approved the high recyclability of adsorbents based on MOF. Hence, the recoverability of adsorbents (FP, TH@FP, MIL@FP and MIL@TH@FP) was studied up to five cycles. The adsorbed metals were removed from the adsorbents by dissolving in acid and the recoverable adsorbents were applied in the second adsorption cycle. The recovering/recycling process was repeated for five consecutive cycles and adsorption results were presented in Fig. S7. Depending on the number of cycles, regardless to the type of the applied absorbent and metal

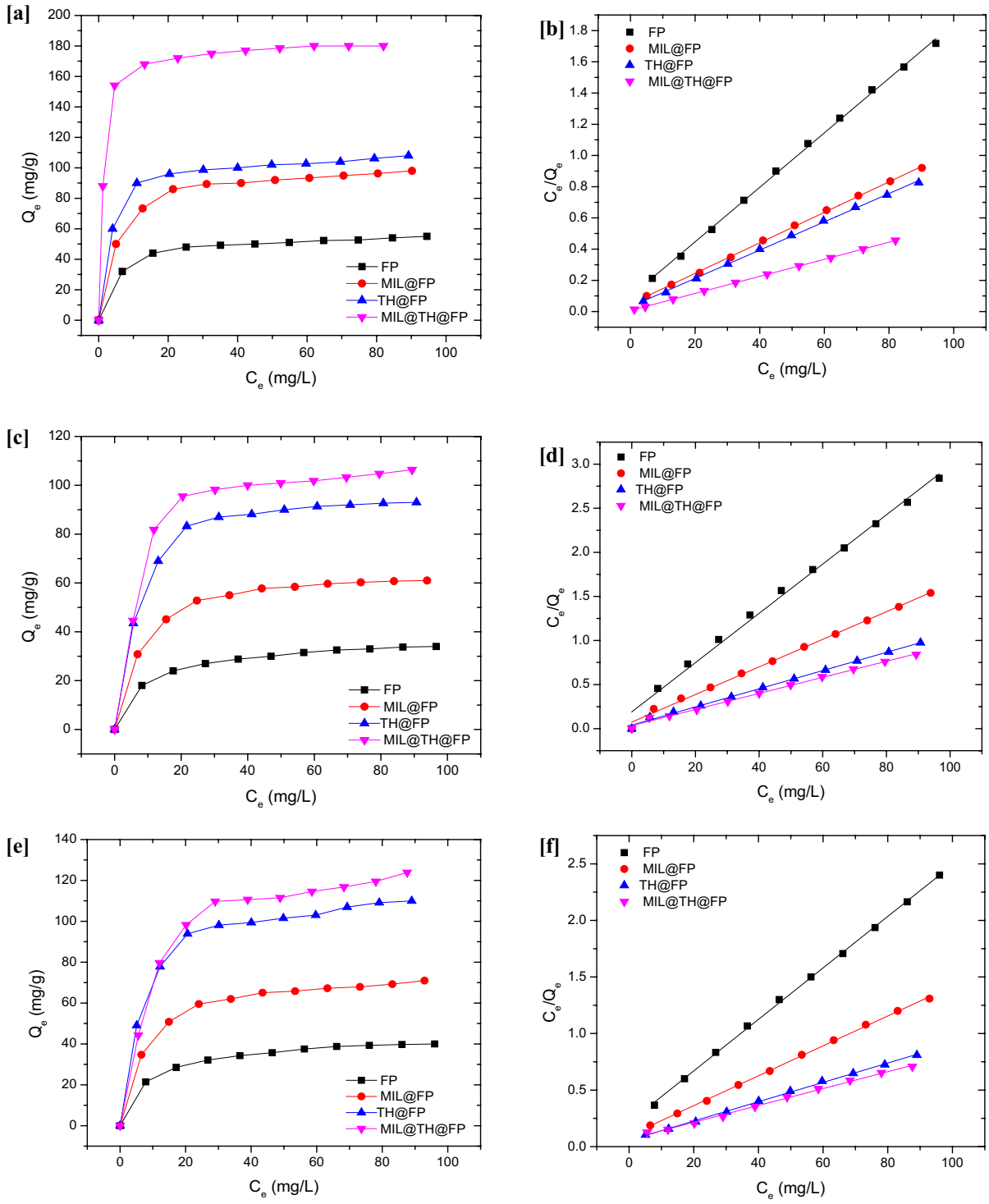

Fig. 6 Adsorption isotherm of metals onto the synthesized materials; **a**, **b** Hg^{+2}, **c**, **d** Cr^{+3}, **e**, **f** Cu^{+2}, **a**, **c**, **e** effect of initial concentration and **b**, **d**, **f** linear fitting for Langmuir model.

Table 2 Isotherm parameters for metal adsoprtion onto the synthesized materials

Metal ions	Samples	Freundlich isotherm			Langmuir isotherm		
		n	K_F	R^2	Q_m (mg/g)	K_L ($\times 10^3$, mg/L)	R^2
Hg^{+2}	FP	5.59	3.22	0.88	57.27	178.97	0.99
	MIL@FP	4.83	3.71	0.86	102.35	198.26	0.99
	TH@FP	6.27	4.00	0.82	110.37	290.39	0.99
	MIL@TH@FP	7.01	4.64	0.75	182.81	821.32	0.99
Cr^{+3}	FP	2.43	4.01	0.97	35.79	146.99	0.99
	MIL@FP	3.09	4.15	0.87	63.86	211.39	0.99
	TH@FP	3.53	4.12	0.81	96.90	260.80	0.99
	MIL@TH@FP	3.62	3.96	0.72	109.65	259.17	0.99
Cu^{+2}	FP	2.63	4.12	0.96	43.94	106.02	0.99
	MIL@FP	3.21	4.12	0.89	75.64	113.53	0.99
	TH@FP	3.47	4.01	0.85	117.10	134.98	0.99
	MIL@TH@FP	3.65	3.13	0.83	134.05	154.01	0.99

ions, for either MIL@TH@FP or any of the prepared materials, the adsorption capacities were gradually decreased as a function of recycling. In case of FP, after five repetitive cycles, the capacities of adsorption were lowered from 50 to 38 mg/g for Hg^{+2}, from 30 to 18 mg/g for Cr^{+3} and from 35 to 22 mg/g for Cu^{+2}. The adsorption capacity of Hg^{+2}, Cr^{+2} and Cu^{+2} was decreased from 175, 101 and 110 mg/g to 135 mg/g, 88 mg/g and 88 mg/g for MIL@TH@FP composite, respectively, after reusing five cycles. Regardless to the metal ion, the adsorption capacities were reduced by 24.0–40.0 and 12.8–22.8% by using FP and MIL@TH@FP, respectively. Comparing to the untreated FP, the synthesized MIL@TH@FP composite showed lower decrement in adsorption capacities of metals after recycling. These data reflected the recyclability and stability of composites is higher compared to the untreated FP. In FP, the occupied active sites of FP (OH) with metal ions were not fully removed during recyclability. This approves the good durability of MIL@TH@FP composite against the recoverability process and consequently maximized the efficiency of heavy metal adsorption.

Tentative mechanism of heavy metals adsorption

The mechanism of heavy metals adsorption could be elucidated according to different studies that were reported in literature (Liu et al. 2021; Pei et al. 2021; Zhao et al. 2019). Meanwhile, the adsorption of Hg^{2+}, Cr^{3+} and Cu^{2+} onto the applied adsorbents (FP, TH@FP, MIL@FP and MIL@TH@FP) was confirmed via SEM micrographs, FTIR spectra, adsorption isotherm and kinetics studies. The adsorption mechanism could be assumed in agreement with the adsorption results and chemical structures of reactants ($Hg^{2+,}$ Cr^{3+}, Cu^{2+}, MIL-125-NH_2, thiophene-2-carboxylic acid and cellulosic FP), as represented in Fig. 7. MIL@TH@FP composite contains many accessible sites represented in functional groups of MIL-125-NH_2 (Ti, OH and NH_2), cellulosic FP (OH) and thiophene-2-carboxylic acid (S and COOH), in addition to the porosity of MIL-125-NH_2. Therefore, metal ions (Hg^{2+}, Cr^{3+} and Cu^{2+}) could be chemically adsorbed onto the composite via coordinative bonding between the as-mentioned functional groups of the exploited composite and the metal ions (Emam et al. 2018). Moreover, the physical deposition of metal ions into the pores of MIL-125-NH_2 and/or FP may be occurred with minor relevant (Abdelhameed et al. 2016, 2017; Emam et al. 2018). This suggestion supported by the obtained results of the highest adsorption capability of MIL@TH@FP composites and the lowest adsorption capacity of FP (Fig. 7). These results are explained by the higher and numerous functional groups inserted in FP by grafting with thiophene and MIL-125-NH_2. Subsequently, the current results reflected the superiority of grafting onto FP for the significant removal of metals.

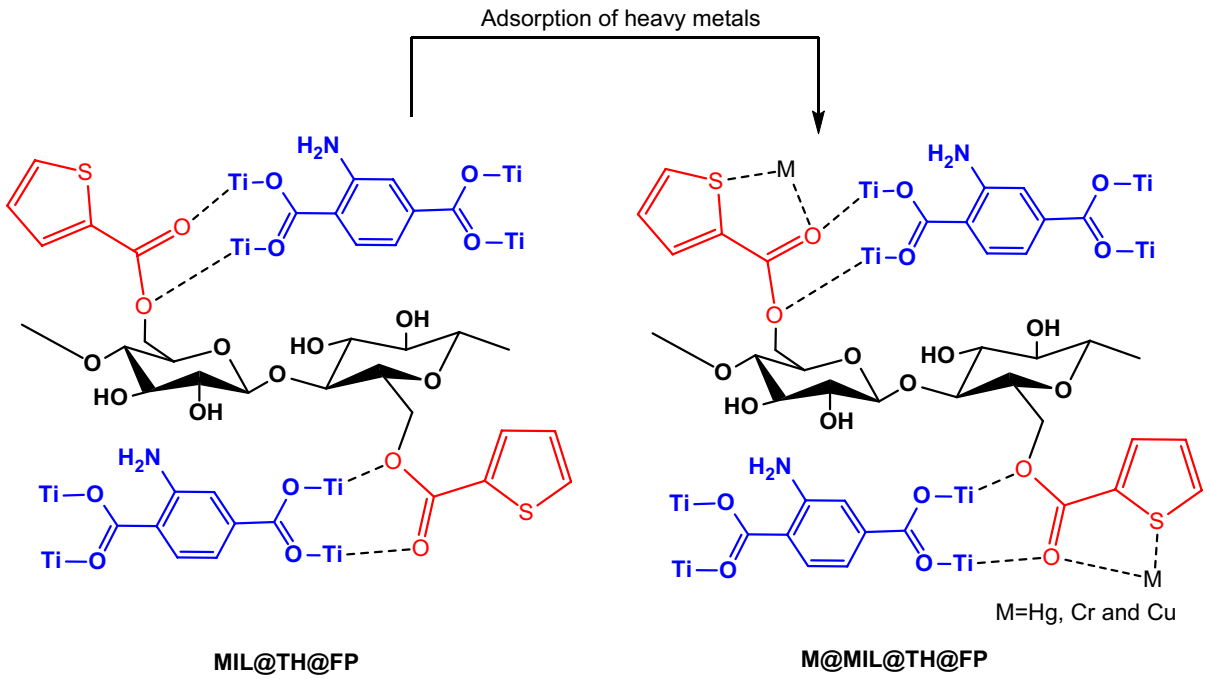

Fig. 7 The suggested adsorption mechanism of metals onto the synthesized composite

Conclusion

Removing of heavy metals from wastewater was carried out in the current work using composite from MIL-125-NH_2 and modified cellulosic FP. FP was preliminary functionalized with thiophene-2-carboxylic acid, and subsequently MIL-125-NH_2 was grafted with the modified FP to prepare MIL@TH@FP composite. The as-prepared materials TH@FP, MIL@FP and MIL@TH@FP composite were characterized by SEM, EDX, XRD and FTIR. The all-formed materials were applied in adsorption of heavy metal (Hg^{2+}, Cr^{3+}, Cu^{2+}) for wastewater treatment. The adsorption of metals was fitted to Langmuir and pseudo-second ordered model. The maximum capacity of metal adsorption onto MIL@TH@FP composite was 182.8, 109.7 and 134.1 for Hg^{+2}, $Cr^{+3}$and Cu^{+2} mg/g, respectively. Compared to Cr^{+3} and Cu^{+2}, the adsorbed amount of Hg^{+2} was significantly high due to the higher affinity of thiophene towards Hg^{+2}. MIL@TH@FP composite showed good recyclability and the metal adsorption capacity was diminished by 12.8–22.8% by five reusing cycles. Such prepared MIL@TH@FP as a recoverable composite could be highly applicable for purification of wastewater from heavy metals with high affinity against mercury ions and could be used for repeated cycles with substantial adsorption affinity.

Acknowledgments Princess Nourah bint Abdulrahman University Researchers Supporting Project number (PNURSP2023R122), Princess Nourah bint Abdulrahman University, Riyadh, Saudi Arabia.

Author contributions All authors conceived of the presented idea. Dr. AMM, Dr. NAA and SFI carried out the experimental work and performed the analytic calculations. Dr HA and Dr. MA figured out the data and presented the data and discussed the results. Prof. FAS and Prof. NME supervised the findings of the work and wrote the manuscript.

Funding This work is funded from Ministry of Education in Saudi Arabia.

Data availability All data generated or analyzed during this study are included in this published article (and its supplementary information files).

Declarations

Conflict of interest The authors declare that they have no competing financial interest.

Consent for publication Authors give their consent for the publication of identifiable details, which can include photo-

graphs and/or details within the text (material) to be publish in this journal.

Ethics approval and consent to participate This work does not contain any studies with human participants or animals performed by any of the authors.

References

Abdelhameed RM, Abdel-Gawad H, Elshahat M, Emam HE (2016) Cu–BTC@ cotton composite: design and removal of ethion insecticide from water. RSC Adv 6:42324–42333

Abdelhameed RM, Emam HE, Rocha J, Silva AM (2017) Cu-BTC metal–organic framework natural fabric composites for fuel purification. Fuel Process Technol 159:306–312

Abdelhameed RM, Rehan M, Emam HE (2018) Figuration of Zr-based MOF@ cotton fabric composite for potential kidney application. Carbohydr Polym 195:460–467

Abdelhameed RM, El-Shahat M, Emam HE (2020) Employable metal (Ag and Pd)@ MIL-125-NH2@ cellulose acetate film for visible-light driven photocatalysis for reduction of nitro-aromatics. Carbohydr Polym 247

Ahluwalia SS, Goyal D (2007) Microbial and plant derived biomass for removal of heavy metals from wastewater. Bioresour Technol 98:2243–2257

Ahmed HB, Emam HE (2016) Layer by layer assembly of nanosilver for high performance cotton fabrics. Fibers Polym 17:418–426

Aksu Z (2005) Application of biosorption for the removal of organic pollutants: a review. Process Biochem 40:997–1026

Annenkova V, Andreyeva N, Annenkova V, Abzayeva K, Voronkov M (1984) Dehydropolycondensation of thiophenol catalysed by MoCl5 and WCl6. Polym Sci USSR 26:953–956

Bakhtiari N, Azizian S (2015) Adsorption of copper ion from aqueous solution by nanoporous MOF-5: a kinetic and equilibrium study. J Mol Liq 206:114–118

Bolster CH, Hornberger GM (2007) On the use of linearized Langmuir equations. Soil Sci Soc Am J 71:1796–1806

Cui L, Wang Y, Gao L, Hu L, Yan L, Wei Q, Du B (2015) EDTA functionalized magnetic graphene oxide for removal of Pb(II), Hg(II) and Cu(II) in water treatment: adsorption mechanism and separation property. Chem Eng J 281:1–10

Dehghankar M, Mohammadi T, Moghadam MT, Tofighy MA (2021) Metal–organic framework/zeolite nanocrystal/polyvinylidene fluoride composite ultrafiltration membranes with flux/antifouling advantages. Mater Chem Phys 260:124128

Emam HE, Abdelhameed RM (2017) In-situ modification of natural fabrics by Cu-BTC MOF for effective release of insect repellent (N,N-diethyl-3-methylbenzamide). J Porous Mater 24:1175–1185

Emam HE, Abdelhameed RM (2017) Anti-UV radiation textiles designed by embracing with nano-MIL (Ti, In)–metal organic framework. ACS Appl Mater Interfaces 9:28034–28045

Emam HE, Bechtold T (2015) Cotton fabrics with UV blocking properties through metal salts deposition. Appl Surf Sci 357:1878–1889

Emam HE, El-Rafie M, Ahmed HB, Zahran M (2015) Room temperature synthesis of metallic nanosilver using acacia to impart durable biocidal effect on cotton fabrics. Fibers Polym 16:1676–1687

Emam HE, Rehan M, Mashaly HM, Ahmed HB (2016) Large scaled strategy for natural/synthetic fabrics functionalization via immediate assembly of AgNPs. Dyes Pigments 133:173–183

Emam HE, Ahmed HB, Bechtold T (2017a) In-situ deposition of Cu_2O micro-needles for biologically active textiles and their release properties. Carbohydr Polym 165:255–265

Emam HE, El-Hawary NS, Ahmed HB (2017b) Green technology for durable finishing of viscose fibers via self-formation of AuNPs. Int J Biol Macromol 96:697–705

Emam HE, El-Zawahry MM, Ahmed HB (2017c) One-pot fabrication of AgNPs, AuNPs and Ag–Au nano-alloy using cellulosic solid support for catalytic reduction application. Carbohydr Polym 166:1–13

Emam HE, Abdellatif FH, Abdelhameed RM (2018) Cationization of celluloisc fibers in respect of liquid fuel purification. J Clean Prod 178:457–467

Emam HE, Ahmed HB, Gomaa E, Helal MH, Abdelhameed RM (2020) Recyclable photocatalyst composites based on Ag_3VO_4 and Ag_2WO_4@ MOF@ cotton for effective discoloration of dye in visible light. Cellulose 27:7139–7155

Fila K, Grochowicz M, Podkościelna B (2018) Thermal and spectral analysis of copolymers with sulphur groups. J Therm Anal Calorim 133:489–497

Hoseinzadeh H, Hayati B, Ghaheh FS, Seifpanahi-Shabani K, Mahmoodi NM (2021) Development of room temperature synthesized and functionalized metal–organic framework/graphene oxide composite and pollutant adsorption ability. Mater Res Bull 142

Hussain AZ, Sheriff KM (2014) Removal of heavy metals from wastewater using low cost adsorbents. Arch Appl Sci Res 6:52–54

Jayaweera H, Siriwardane I, de Silva K, de Silva RM (2018) Synthesis of multifunctional activated carbon nanocomposite comprising biocompatible flake nano hydroxyapatite and natural turmeric extract for the removal of bacteria and lead ions from aqueous solution. Chem Cent J 12:1–14

Ke F, Qiu L-G, Yuan Y-P, Peng F-M, Jiang X, Xie A-J, Shen Y-H, Zhu J-F (2011) Thiol-functionalization of metal–organic framework by a facile coordination-based post-synthetic strategy and enhanced removal of Hg^{2+} from water. J Hazard Mater 196:36–43

Li G-P, Zhang K, Zhang P-F, Liu W-N, Tong W-Q, Hou L, Wang Y-Y (2019) Thiol-functionalized pores via post-synthesis modification in a metal–organic framework with selective removal of Hg(II) in water. Inorg Chem 58:3409–3415

Liang L, Chen Q, Jiang F, Yuan D, Qian J, Lv G, Xue H, Liu L, Jiang H-L, Hong M (2016) In situ large-scale construction of sulfur-functionalized metal–organic framework and its

efficient removal of Hg(II) from water. J Mater Chem A 4:15370–15374
Liu T, Che JX, Hu YZ, Dong XW, Liu XY, Che CM (2014) Alkenyl/thiol-derived metal–organic frameworks (MOFs) by means of postsynthetic modification for effective mercury adsorption. Chem A Eur J 20:14090–14095
Liu B, Pei L, Zhao X, Zhang X, Huang H (2021) Synergistic dual-pyrazol sites of metal–organic framework for efficient separation and recovery of transition metals from wastewater. Chem Eng J 410
Luo Y, Li B, Wang W, Wu K, Tan B (2012) Hypercrosslinked aromatic heterocyclic microporous polymers: a new class of highly selective CO2 capturing materials. Adv Mater 24:5703–5707
Luo F, Chen JL, Dang LL, Zhou WN, Lin HL, Li JQ, Liu SJ, Luo MB (2015) High-performance Hg2+ removal from ultra-low-concentration aqueous solution using both acylamide-and hydroxyl-functionalized metal–organic framework. J Mater Chem A 3:9616–9620
Madadrang CJ, Kim HY, Gao G, Wang N, Zhu J, Feng H, Gorring M, Kasner ML, Hou S (2012) Adsorption behavior of EDTA-graphene oxide for Pb(II) removal. ACS Appl Mater Interfaces 4:1186–1193
Mahmoodi NM, Saffar-Dastgerdi MH (2019) Zeolite nanoparticle as a superior adsorbent with high capacity: synthesis, surface modification and pollutant adsorption ability from wastewater. Microchem J 145:74–83
Mahmoodi NM, Arabloo M, Abdi J (2014) Laccase immobilized manganese ferrite nanoparticle: synthesis and LSSVM intelligent modeling of decolorization. Water Res 67:216–226
Mon M, Lloret F, Ferrando-Soria J, Martí-Gastaldo C, Armentano D, Pardo E (2016) Selective and efficient removal of mercury from aqueous media with the highly flexible arms of a BioMOF. Angew Chem 128:11333–11338
Mon M, Bruno R, Tiburcio E, Viciano-Chumillas M, Kalinke LH, Ferrando-Soria J, Armentano D, Pardo E (2019) Multivariate metal–organic frameworks for the simultaneous capture of organic and inorganic contaminants from water. J Am Chem Soc 141:13601–13609
Nguyen T, Ngo H, Guo W, Zhang J, Liang S, Yue Q, Li Q, Nguyen T (2013) Applicability of agricultural waste and by-products for adsorptive removal of heavy metals from wastewater. Bioresour Technol 148:574–585
Oehmen A, Vergel D, Fradinho J, Reis MA, Crespo JG, Velizarov S (2014) Mercury removal from water streams through the ion exchange membrane bioreactor concept. J Hazard Mater 264:65–70
Park J-D, Zheng W (2012) Human exposure and health effects of inorganic and elemental mercury. J Prev Med Public Health 45:344
Pei L, Zhao X, Liu B, Li Z, Wei Y (2021) Rationally tailoring pore and surface properties of metal–organic frameworks for boosting adsorption of Dy3+. ACS Appl Mater Interfaces 13:46763–46771
Qasem N, Mohammed R, Lawal D (2021) Removal of heavy metal ions from wastewater: a comprehensive and critical review. Npj Clean Water 4:36
Rajasulochana P, Preethy V (2016) Comparison on efficiency of various techniques in treatment of waste and sewage water—a comprehensive review. Resour Technol 2:175–184
Rice KM, Walker EM Jr, Wu M, Gillette C, Blough ER (2014) Environmental mercury and its toxic effects. J Prev Med Public Health 47:74
Shahid M, Khalid S, Bibi I, Bundschuh J, Niazi NK, Dumat C (2020) A critical review of mercury speciation, bioavailability, toxicity and detoxification in soil–plant environment: ecotoxicology and health risk assessment. Sci Total Environ 711:134749
Sharma S, Bhattacharya A (2017) Drinking water contamination and treatment techniques. Appl Water Sci 7(3):1043–1067
Tesfaye D (2016) Removal of lead from waste water using corn cob activated carbon as an adsorbent. Addis Ababa University, Addis Ababa
Tyagi C, Tomar LK, Singh H (2009) Surface modification of cellulose filter paper by glycidyl methacrylate grafting for biomolecule immobilization: influence of grafting parameters and urease immobilization. J Appl Polym Sci 111:1381–1390
Wang X, Chen L, Wang L, Fan Q, Pan D, Li J, Chi F, Xie Y, Yu S, Xiao C (2019) Synthesis of novel nanomaterials and their application in efficient removal of radionuclides. Sci China Chem 62:933–967
WHO, G (2011) Guidelines for drinking-water quality. World Health Organization, vol 216, pp 303–304
Yee K-K, Reimer N, Liu J, Cheng S-Y, Yiu S-M, Weber J, Stock N, Xu Z (2013) Effective mercury sorption by thiol-laced metal–organic frameworks: strong acid and the vapor phase. J Am Chem Soc 135:7795–7798
Yin WH, Xiong YY, Wu HQ, Tao Y, Yang LX, Li JQ, Tong XL, Luo F (2018) Functionalizing a metal–organic framework by a photoassisted multicomponent postsynthetic modification approach showing highly effective Hg(II) removal. Inorg Chem 57:8722–8725
Zhao X, Wang Y, Li Y, Xue W, Li J, Wu H, Zhang Y, Li B, Liu W, Gao Z (2019) Synergy effect of pore structure and amount of carboxyl site for effective removal of Pb2+ in metal–organic frameworks. J Chem Eng Data 64:2728–2735